The neurological and behavioral consequences of dystrophin deficiency in Duchenne muscular dystrophy: insights from mouse models

Verhaeg, M.A.T.

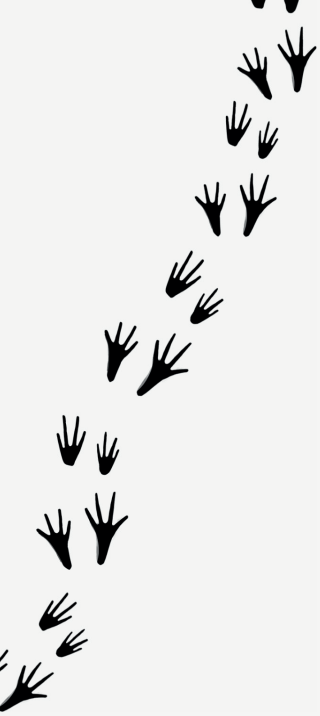

Minou Verhaeg[1], Kevin Adamzek[1], Davy van de Vijver[1], Kayleigh Putker[1], Sarah Engelbeen[1], Daphne Wijnbergen[1], Maurice Overzier[1], Ernst Suidgeest[2], Louise van der Weerd[1,2], Annemieke Aartsma-Rus[1], Maaike van Putten[1].

1: Department of Human genetics, Leiden University Medical Center, Leiden, the Netherlands

2: C.J. Gorter MRI Center, Department of Radiology, Leiden University Medical Center, Leiden, the Netherlands

CHAPTER 3

Learning, memory and blood-brain barrier pathology in Duchenne muscular dystrophy mice lacking Dp427, or Dp427 and Dp140

Genes, Brain and Behavior, 2024. 23(3): p. e12895

Abstract

Duchenne muscular dystrophy is a severe neuromuscular disorder that is caused by mutations in the *DMD* gene, resulting in a disruption of dystrophin production. Next to dystrophin expression in the muscle, different isoforms of the protein are also expressed in the brain and lack of these isoforms leads to cognitive and behavioral deficits in patients. It remains unclear how the loss of the shorter dystrophin isoform Dp140 affects these processes. Using a variety of behavioral tests, we found that *mdx* and *mdx*^{4cv} mice (which lack Dp427 or Dp427 + Dp140, respectively) exhibit similar deficits in working memory, movement patterns and blood-brain barrier integrity. Neither model showed deficits in spatial learning and memory, learning flexibility, anxiety or spontaneous behavior, nor did we observe differences in aquaporin 4 and glial fibrillary acidic protein. These results indicate that in contrast to Dp427, Dp140 does not play a crucial role in processes of learning, memory and spontaneous behavior.

Keywords

Dystrophin, cognition, spontaneous behavior, neuromuscular disease, spatial learning

Summary statement

In mice, Dp427 is involved in learning, memory and spontaneous behavior, while Dp140 does not appear to play a crucial role in these aspects.

Introduction

Duchenne muscular dystrophy (DMD) is a recessive X-linked neuromuscular disorder affecting approximately 1 in 5,000 newborn males (Aartsma-Rus et al. 2016). It is characterized by progressive muscle weakness, eventually leading to premature death in the third or fourth decade of a patient's life due to respiratory and/or cardiac failure (Emery 2002). In addition to the musculature's pathological hallmarks, a significant proportion of DMD patients also presents with cognitive impairments from an early age onwards. The overall intelligence quotient of DMD patients is one standard deviation below the population mean (Hinton et al. 2007, Banihani et al. 2015) and approximately 30% of DMD patients suffer from neuronal disorders or behavioral problems (Billard et al. 1992), including autism spectrum disorder, attention-deficit hyperactivity disorder, inattention, reading deficits, obsessive-compulsive disorder, anxiety, depression and epilepsy (Hinton et al. 2006, Hendriksen and Vles 2008, Waite et al. 2012, Banihani et al. 2015, Ricotti et al. 2016).

DMD is caused by mutations in the *DMD* gene, which prevent synthesis of functional dystrophin protein. The *DMD* gene is the largest known human gene and contains seven unique promotor regions, which give rise to different dystrophin isoforms that are expressed in a tissue and/or cell-specific manner. Only the full-length isoform Dp427m (427 kDa, muscle) is expressed in muscle, whereas five dystrophin isoforms are expressed in the central nervous system (CNS). The full-length isoform Dp427c is predominantly expressed in neurons of the cortex and CA regions of the hippocampus (Nudel et al. 1989, Lidov et al. 1990), while Dp427p is expressed in the cerebellar Purkinje cells (Holder et al. 1996). The shorter isoform Dp140 is expressed in the cerebral cortex in fetal life stages and in the cerebellum postnatally (Doorenweerd et al. 2017). Dp71 and Dp40 are ubiquitously expressed at high levels throughout the CNS (Doorenweerd et al. 2017). The role of the different dystrophin isoforms in the CNS is only partly understood. Dp427 has been suggested to be involved in synapse structure and functioning (Blake and Kröger 2000). Dp140 seems to play a role in pre-synaptic plasticity in the excitatory synapses (Hashimoto et al. 2022). Dp71 is associated with blood-brain barrier (BBB) permeability (Anderson et al. 2012) and synaptic organization (Daoud et al. 2009), while Dp40 plays a possible role in presynaptic function (Tozawa et al. 2012).

Depending on the location of the mutation, DMD patients lack one or multiple dystrophin isoforms, i.e. DMD patients with a mutation in the 5'end of the *DMD* gene only lack the Dp427 isoforms, while those with a mutation in the 3' end of the *DMD* gene either lack Dp427 and Dp140 or all dystrophin isoforms in the CNS. A correlation between the amount of missing isoforms and the severity and incidence of cognitive deficits seems to exist (Taylor et al. 2010, Chamova et al. 2013, Ricotti et al. 2016). However, it is still unclear how the lack of the distinct dystrophin isoforms in the CNS affects cognition, behavior and overall brain pathology.

The consequences of dystrophinopathy on behavior and brain pathology have been studied in several DMD mouse models. *Mdx* mice, which have a point mutation in exon 23 and consequently lack Dp427, have been most thoroughly studied. They show impaired functioning in cognitive processes concerning social behavior (Miranda et al. 2015), spatial and recognition memory (Vaillend et al. 2004), depressive-like behavior (Manning et al. 2014) and anxiety and fear (Sekiguchi et al. 2009, Vaillend and Chaussenot 2017, Comim et al. 2019). Only recently, the consequences of the additional lack of Dp140 have been investigated in the *mdx52* mouse, which have a deletion of exon 52, and *mdx*^{4cv} mice, which have a nonsense mutation in exon 53. Both mouse models show deficits in cognitive processes such as fear and social behavior (Aupy et al. 2020, Zhang et al. 2020, Saoudi et al. 2021). However, direct comparisons between mice lacking only Dp427 and mice lacking Dp427+Dp140 are minimal, making it difficult to understand the exact effects of the lack of Dp140.

To further investigate the consequences of the lack of one or multiple dystrophin isoforms in more detail, we subjected *mdx* and *mdx*^{4cv} mice to behavioral tests and MRI analyses. In working memory related tasks we observed an equally decreased performance in *mdx* and *mdx*^{4cv} mice, while only *mdx* mice showed a delay in spatial learning. *Mdx* and *mdx*^{4cv} mice both displayed increased performance in a food related task and affected movement patterns during spontaneous behavior. No differences were found in memory flexibility or anxiety. Furthermore, *mdx* and *mdx*^{4cv} mice showed similar increases in BBB permeability. Overall, the lack of Dp140 did not seem to have additional effects on different types of memory, spontaneous behavior or BBB function in mice.

Materials and Methods

Mice

Male *mdx* (*mdx*(BL6) *n*=25) (Veltrop et al. 2013), *mdx*^{4cv} (B6Ros.Cg-*Dmd*$^{mdx\text{-}4Cv}$/J *n*=23) (Chapman et al. 1989) and wild type (WT) mice (C57BL/6J *n*= 21), were bred at the animal facility of the Leiden University Medical Center (LUMC). Heterozygous females of each of the DMD strains were paired with WT males to generate DMD and WT males from the same litters. WT mice were taken equally from litters of both strains for experiments, and since no statistical differences were observed between the two, we considered them as one WT group. Mice were housed in individually ventilated cages (Makrolon type II), filled with sawdust and enriched with cardboard nesting material, with 12 hour dark/light cycles. Mice had *ad libitum* access to water and standard RM3 chow (SDS, Essex, United Kingdom). Experiments were performed at the animal facility of the LUMC in rooms dedicated for behavioral experiments. The experiments were approved by the Central Authority for Scientific

Procedures on Animals and conform with the Directive 2010/63/EU of the European Parliament.

Behavioral tests

Experimental setup

Starting between 10 to 15 weeks of age, mice were subjected to a series of experiments spread over a five week period. The experiments consisted of the T-maze, Morris water maze (MWM), and housing in a PhenoTyper automatic home cage for 7 days in which spontaneous behavior, anxiety and discrimination and reversal learning were assessed (Fig. 1).All experiments were performed at the same time of the day. Spontaneous behavior was automatically tracked in the PhenoTyper cages 24h a day. Animal behavior and location were tracked with Ethovision XT, at a rate of 20 frames per second.

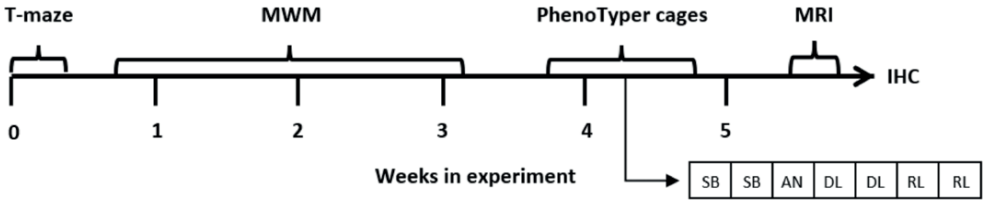

Figure 1: Overview of the experimental setup. *Mice started between 10 to 15 weeks of age and underwent testing via T-maze, Morris water maze (MWM), PhenoTyper cages and a series of MRI scans. SB: spontaneous behavior. AN: anxiety. DL: discrimination learning. RL: reversal learning.*

T-maze

After two days of handling, a T-maze (white PVC, arms 30x10x25cm) was used to assess spatial working memory of the mice. During the learning trial, mice were released in the start arm and given 60 seconds to enter one of the goal arms. A door was lowered upon entering the goal arm and the mouse was maintained there for 30 seconds before it was removed from the maze. The test trial was performed directly after the learning trial. Here, the mouse was contained in the start location for 10 seconds after which it was allowed to walk through the maze for 60 seconds. In total, six learning and test trials were executed over a period of two days, with at least one hour rest in between tests. Four *mdx* and four *mdx*^{4cv} mice were excluded because they did not complete the trials.

Morris water maze

The MWM was used to assess the spatial- and reversal learning. The MWM consists of a circular pool (diameter = 120cm) filled with dyed, non-transparent water. The maze contains a platform (diameter = 11cm) located just below the surface of the water, half way between the center of the pool and the wall. Three distinct distal cues located outside the maze allowed mice to navigate through the pool. The test protocol consisted of an acquisition- and reversal learning phase. The acquisition trials, in which mice learned to locate the hidden platform, were conducted over a period of five days, with four trials per day. Hereto, the platform was located in the north-west quadrant of the pool and starting positions of mice were semi-randomly allocated according to the strategy in Vorhees et al. (Vorhees and Williams 2006). If the animal failed to locate the platform within two minutes, it was placed onto the platform, where it was allowed to stay for 15 seconds before being taken out. Three days after the last acquisition phase, a probe trial was performed, during which the platform was removed and swimming behavior was monitored for two minutes.

In the reversal learning phase, the platform was relocated in the south-east quadrant and swimming behavior was recorded for two minutes, or until the platform was reached. Trials were performed in a similar manner as in the acquisition phase, but included four days instead of five, after which a probe trial was conducted.

PhenoTyper automated home-cages

A PhenoTyper automated home-cage (Noldus PhenoTyper 3000, Noldus Information Technology), with transparent Perspex walls (30x30x35cm) and opaque Perspex floor, was used to assess the mice's behavior. The home-cage included sawdust bedding and was equipped with a drinking and feeding station. A rectangular shelter (10x10x5cm) with two entrances (diameter 3cm) was fixed in one corner. An infrared camera was mounted in the top.

Spontaneous behavior

Mice were put into the automated home-cages during the light phase (5-9h after the start of the light phase) with *ad libitum* access to water and standard RM3 chow. Mice were individually housed and the location of the mice (middle of the body) was continuously tracked for 48 hours, starting from the first dark phase. Twenty parameters for spontaneous behavior were calculated from the automatic tracked location of the mice and analyzed as described by Loos et al. for the dark and light phase of day 2 (Loos et al. 2014). Since automatic tracking was successful for all the mice, no manual scoring was necessary. Due to the 24h tracking system of the

PhenoTyper cages, the exact same time windows could be used for all the mice. Furthermore, total distance and velocity were analyzed as an indicator for muscle function. Two *mdx* mice and one *mdx*^{4cv} mouse were excluded from analyses due to a technical issue with their recordings. We did not have to exclude mice based on their sleeping behavior, since none of them slept outside their shelter (exclusion criteria of Loos et al. (Loos et al. 2014)).

Anxiety test

An anxiety test was conducted to examine the behavioral response of the mice to an external trigger, i.e. a bright light-emitting diode (LED) spot (Aarts et al. 2015). A bright LED light (700 lux) was automatically activated for the duration of 1 hour, 75 minutes after the start of the third dark phase (20.15h local time at the animal facility). The LED light was positioned between the feeding station and the left shelter entrance. Time spent outside the shelter was calculated per block of 15 minutes for a duration of 2 hours and 15 minutes (20.00 till 22.15 local time at animal facility). Two *mdx* mice and one *mdx*^{4cv} mouse were excluded from analyses due to a technical issue with their recordings.

Discrimination and reversal learning task

On the fourth day, *ad libitum* standard chow was removed and an opaque Perspex wall with three entrances (17 cm wide, 25 cm high, 3 cm diameter holes) was placed in front of a pellet dispenser tube which protruded through the corner opposite of the shelter (Remmelink et al. 2016). Water was accessible *ad libitum* during the entire behavioral trial. During the two-day discrimination learning phase, the mice received one food pellet (Dustless Precision Pellets, 14 mg, Rodent Purified diet, Bio Serv, Frenchtown, NJ, USA) after five entries through the left hole of the cognition wall, which did not have to be consecutive. Directly thereafter, two days of reversal learning were initiated in which the target hole changed from the left to the right hole.

Discrimination and reversal learning was defined as the total number of entries needed to reach a 80% criterion of correct entries. This was calculated via a moving window of 30 entries.

After completion of the trials, mice were transferred back to individually ventilated cages with *ad libitum* access to water and standard RM3 chow. Mice were housed individually for the remainder of the study.

Magnetic resonance imaging analyses

MRI scans were generated from 10 randomly selected mice per strain using a 7T Bruker PharmaScan system (Bruker Biospin, Ettlingen, Germany). Mice were anesthetized with isoflurane (4% induction and 1.5% maintenance) after which an intraperitoneal canula was placed. Thereafter, mice were fixed onto the bed with ear bars and a tooth-bar, and an RF-coil was placed over the head of the mice. A water-heated thermos-coupled pad placed underneath the mice was used to control the body temperature with a rectal probe. Throughout the MRI scans, respiratory rate and body temperature were monitored.

MRI scans included a localizer scan and a T2-weigthed Turbo RARE scan to determine volumes of the total brain and brain regions (echo time 39 ms, repetition time 2345.121 ms, averages 12, repetition 1, echo spacing 13 ms, RARE factor 8, slice thickness 0.7 mm, 19 slices, image size 250x208 mm, field of view 18x15 mm). Dynamic contrast-enhanced MRI (DCE-MRI) was done using T1-weighted RARE scans to determine BBB integrity (echo time 13.2 ms, repetition time 700 ms, averages 8, repetition 1, echo spacing 6.6 ms, RARE factor 4, slice thickness 0.5 mm, 19 slices, image size 196x196 mm, field-of-view 18x15 mm). After the first T1W RARE scan, the protocol was interrupted and mice were injected with 100 µl of contrast solution (ProHance Gadoteridol, Bracco diagnostics Inc., NJ, USA- produced by BIPSO, Singen, Germany), through the intraperitoneal canula before resuming the remaining six T1W RARE scans acquired over 42 minutes. To determine regions of interest, data was segmented using an atlas with 23 brain regions (Lein et al. 2007, Boehm-Sturm et al. 2017, Huebner et al. 2017, Koch et al. 2019).Data acquisition, image reconstruction and visualization were performed with Paravision 6.0.1. software (Bruker Biospinm Ettlingen, Germany). The time course of the signal intensity changes was used for statistical analyses.

Sectioning and aquaporin 4 staining

After the MRI scans, mice were sacrificed by CO_2 without recovery from anesthesia. The brain was isolated and immediately frozen by covering it with dry ice powder. All samples were stored at -80^{o}C. Coronally oriented sections (12 µm thick) were generated with a cryostat and stored at -80^{o}C. Before staining, slides were washed with 0.1 M phosphate-buffered saline (PBS) and blocked with a mixture of 5% goat serum (Sigma-Aldrich, cat no. G9023-10ML) and 0.1% Triton X-100 (sigma-Aldrich cat. No. T9284-500ML) for 1 hour. Tissue sections were incubated with primary antibody (anti-aquaporin 4, Sigma-Aldrich, AB3594-50UL, diluted 1:500 and anti-GFAP, ThermoFisher, 13-0300, 1:250, diluted in PBS with 0.1% Triton and 1% goat serum) overnight. Sections were washed and incubated with secondary antibody (donkey

anti-rabbit, ThermoFisher, A-21207 and donkey anti-rat, ThermoFisher, A-21208, both 1:250, diluted in PBS with 0.1% Triton and 1% goat serum) for 45 minutes and cover slipped with ProLong Gold mounting medium with DAPI (Invitrogen, cat. No. P36931). Images were made with a Zeiss AxioScan slide scanner at a 20 times magnification. Three sections per mouse were stained and scanned and one optimal section was selected via visual inspection, based on similarity in location within the brain, and minimal freezing damage or interference from other artifacts. Fluorescence images were converted into gray scales and intensities were determined in the cortex and hippocampus regions on one image per mouse using mean gray value in ImageJ. Analyses were done on one hemisphere. The ROI in the cortex was located close to the longitudinal fissure (Fig 7). For each image, data was then normalized against background levels, which were determined per image at 3 locations within the original ROI to account for difference in intensity caused by the imaging.

Data analysis

All data were checked for normality and equal variance. See table S1 for an overview of the tests per parameter. F- and t-values corresponding to significant *P* values can be found in table S2.In case of normality and equal variance, group differences were determined by Tukey HSD tests. Comparisons with chance levels were made via a one sample t-test per group. If normality and equal variance was not met, Kruskal-Wallis tests were performed and if significant, additional Mann-Whitney repeated tests were performed. Comparisons to chance levels were made with a one-sample Wilcoxon signed-rank test per group. Linear mixed models were used to assess time and strain differences for acquisition and reversal learning in the MWM and to assess for strain and time differences in baseline and in anxiety condition in the anxiety test in the PhenoTypers. These analyses were performed in Rstudio (version 4.3.1) using the LmerTest package (version 3.1.3). Discrimination- and reversal learning in the PhenoTypers was tested with the Martel-Cox test. Multiple comparison corrections were applied to the parameters of spontaneous behavior and the MRI scans using false discovery rate (FDR). All data is presented as mean ± standard error of the mean (SEM). *: $P<0.05$, **: $P<0.01$, ***:$P<0.001$.

Results

DMD mice show decreased but not fully impaired performance in a working memory task

To assess spatial working memory, spontaneous alternation was measured with the T-maze (Fig. 2A). Spontaneous alternation was defined as entering the previously uninvestigated lateral arm of the T-maze (Lalonde 2002).

Both *mdx* and *mdx*^{4cv} mice showed lower levels of spontaneous alternation compared to WTs (P<0.001 and P=0.007 respectively). However, spontaneous alternation was still above chance level of 50% in *mdx* (P=0.017) and *mdx*^{4cv} (P<0.001) mice, suggesting that their spatial working memory was not fully impaired. Mice performance did not differ significantly between different trials, suggesting a minimal effect of repeated exposure (Fig. 2B).

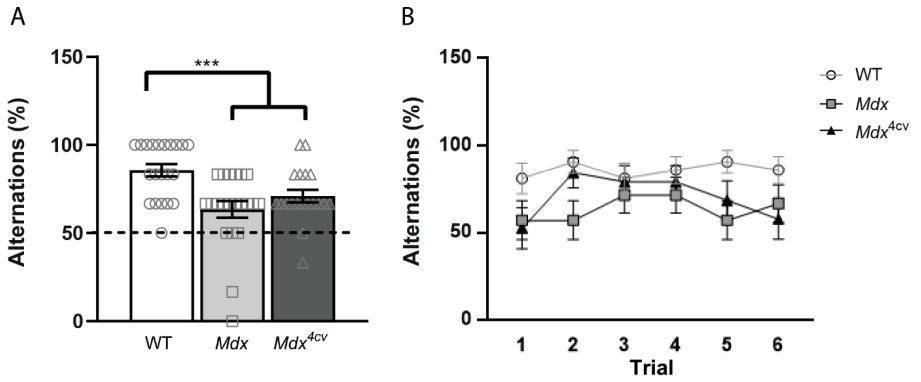

Figure 2: T-maze spontaneous alternation for WT (n=21), mdx (n=21) and mdx^{4cv} (n=19) mice. *A) Lower levels of spontaneous alternation were observed in mdx and mdx^{4cv} compared to WT mice. Chance level is indicated by the dotted line. B) Alterations per trial did not differ between strains. Asterisks indicate *** P<0.001.*

Delay in spatial learning only visible in mdx mice in Morris water maze

As Dp140 is thought to play a role in synaptic plasticity, which is a key player in mechanisms underlying learning and memory, we hypothesized that lack of Dp140 could negatively affect learning capabilities for both forward and reversal learning. The MWM was used to asses spatial reference memory. During acquisition, all strains showed the ability to learn the location of the platform as indicated by a significant effect of trial day on the distance to reach the platform (P<0.001). *Mdx* mice

had a lower learning speed compared to WT (P=0.002) and *mdx*^{4cv} mice (P=0.003) (Fig. 3A) Learning was measured in terms of distance swam instead of latency, due to the differences found in swimming velocity, to minimize the influence of muscle functionality on the task outcomes. Interestingly, only *mdx* mice showed lower maximum swimming velocity when compared to both WT and *mdx*^{4cv} mice (both P<0.001) (Fig. 3B). During the probe test, in which the platform was removed, no differences were found between groups for distance swam to reach the platform zone (Fig. 3C).

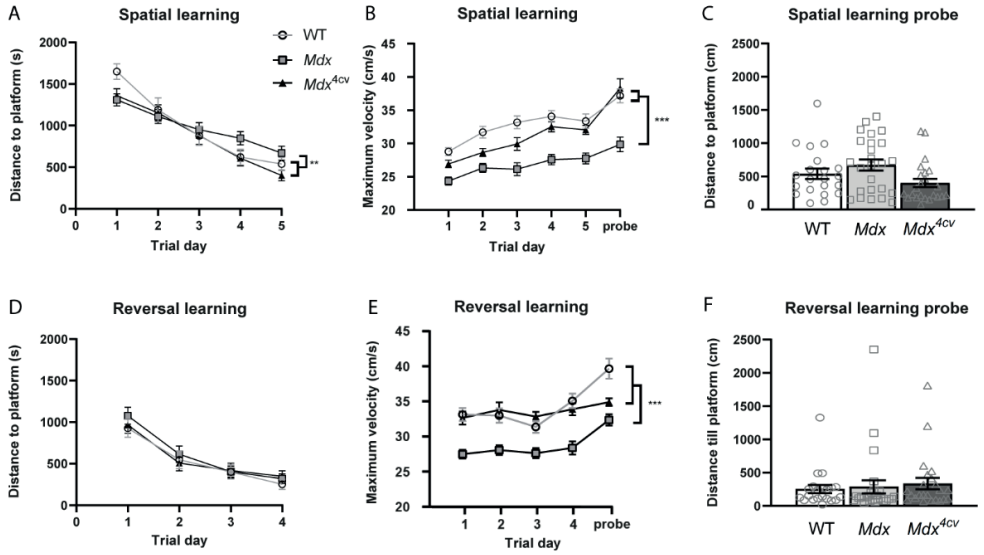

Figure 3: Morris water maze spatial and reversal learning for WT (n=21), mdx (n=25) and mdx^{4cv} (n=23) mice. *A) Distance to platform average of all trials per day. All mice had the capacity to learn the platform location as indicated by the decrease in average distance required to locate the platform. Mdx mice had a decreased learning speed compared to WT and mdx^{4cv} mice. B) Maximum swim velocity was significantly lower in mdx compared to WT and mdx^{4cv} mice. C) Average distance swam to reach the platform zone during the probe trial. D) Distance to platform average of all trials per day. All mice had a comparable capacity to learn the new platform location as indicated by the decrease in average distance swam to the platform. E) Maximum swim velocity was significantly lower in mdx compared to WT and mdx^{4cv} mice. F) Average distance swam to reach the platform zone durin g the probe trial. Asterisks indicate ** P<0.01, *** P<0 .001.*

Unlike forward learning, reversal learning requires the animals to be flexible and adjust their previous learned knowledge and behavior (Izquierdo et al. 2017). By changing the conditions of the earlier established task, cognitive flexibility was assessed. During these reversal learning trials, in which mice had to find the new

platform location, no differences were found in the distance travelled to reach the platform (Fig. 3D). Also here, maximum swimming velocity was significantly lower in *mdx* compared to WT mice and *mdx*^{4cv} (both P<0.001) (Fig. 3E). During the reversal probe, no significant differences were observed in distance swam to reach the platform zone (Fig. 3F).

DMD mice outperform WTs in food rewarded discrimination, but not in reversal learning

To further assess different aspects of memory, the PhenoTyper cages were used to perform a food driven discrimination and reversal learning task. The amount of entries needed to reach an 80% success rate was calculated per mouse on a 30 entry window for both discrimination-, and reversal learning trials. Survival curves were calculated and compared between groups (Fig. 4A,B). During discrimination learning, *mdx* (P=0.032) and *mdx*^{4cv} (P=0.006) mice reached the 80% criterium faster than WTs. No significant differences were found during the reversal learning in the amount of entries or neutral and perseverative errors (data not shown).

No differences in light induced anxiety related behavior in DMD mouse models

During the third night in the PhenoTyper cages, a bright light was illuminated to assess the anxiety reaction in the mice. Time spent outside the shelter was measured in 15 minute bins starting 15 minutes before the light went on (phase 1), during the light exposure (phase 2) and for 1 hour after the light was turned off (phase 3). Measurements were compared to baseline levels of the strain 24h earlier. All groups reacted to the light stimulus with decreased time spent outside the shelter (WT: P<0.001, *mdx*: P<0.001 and *mdx*^{4cv}*:* P=0.002), but no differences were found between groups (Fig. 4C) due to the plateau reaction in WT mice.

Activity and movement related parameters of spontaneous behavior are affected in both DMD models

To assess different aspects of spontaneous behavior such as activity, changes before and during light switches and movement and arrest patterns, 20 parameters were assessed as described by Loos et al (Loos et al. 2014) (Table S3). To determine the possible influence of decreased muscle functionality on spontaneous behavior, the average walking velocity was assessed during the 2nd light and dark phase in the

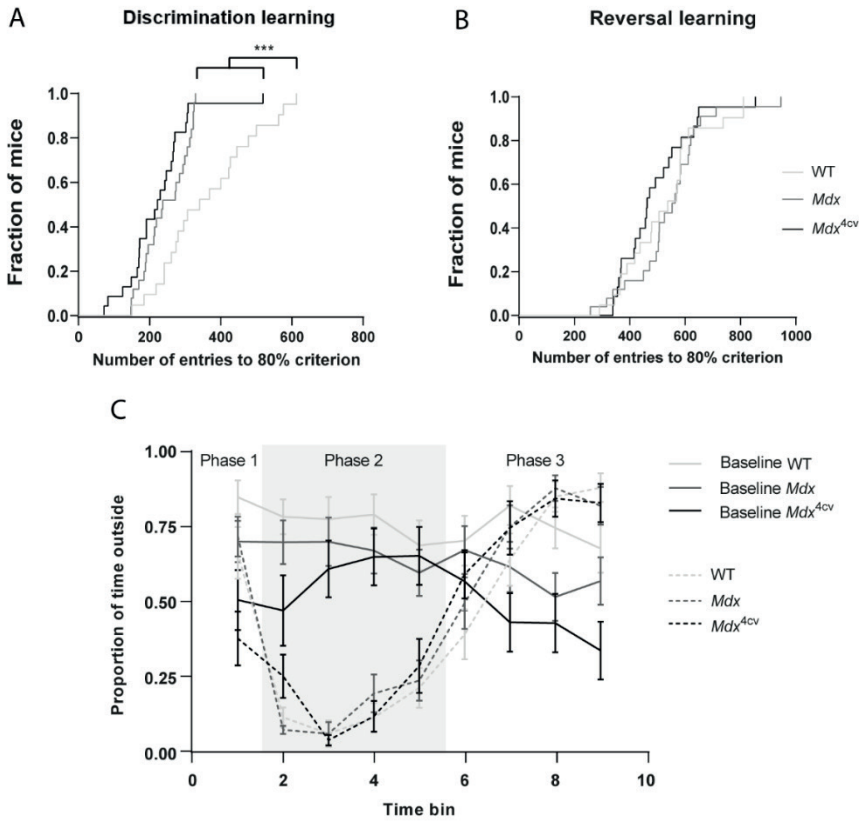

Figure 4: Discrimination- and reversal learning with cognition wall and anxiety in PhenoTyper cages for WT (n=21), mdx (n=23-25) and mdx^{4cv} (n=22-23) mice. *80% success rate was calculated over a time window of 30 entries. A) Survival curve of discrimination learning trials. Mdx and mdx^{4cv} mice were significantly faster in reaching the 80% criterium than WTs during discrimination learning. B) Survival curves of reversal learning trials. No differences were found between groups. C). Grey area (phase 2) represents the time the light was on. All groups showed a significant response to the light in phase 2 compared to baseline measurements of 24h earlier. No differences were found between groups in the anxiety response.* Asterisks

PhenoTyper cages (Fig. 5A). *Mdx* mice, but not *mdx^{4cv}* mice, had decreased walking velocity in the dark phase compared to WT mice (*P*=0.012). Overall activity patterns were furthermore affected in the DMD mouse models (Fig. 5B-C). During the dark phase overall activity was lower in both *mdx* (*P*=0.008) and *mdx^{4cv}* mice (*P*=0.015) compared to WTs (Fig. 5B). Additionally, the extent to which overall activity was changed during the last two hours of the light phase (anticipation of the dark phase) was lower in both *mdx* and *mdx^{4cv}* mice compared to WTs (*P*=0.001 and *P*=0.041 respectively) (Fig. 5C).

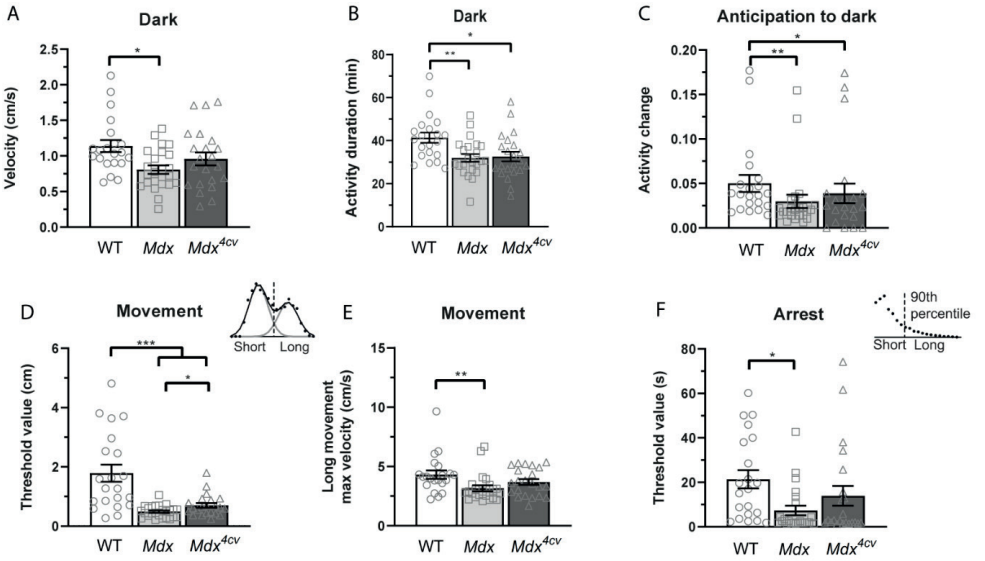

Figure 5: Spontaneous behavior in PhenoTyper cages for WT (n=21), mdx (n=23) and mdx^{4cv} (n=22) mice. *A) Average velocity was lower in mdx mice compared to WT mice during the dark phase. B) The duration of active behavior was shorter in both DMD models compared to WTs in the dark phase. C) Mdx and mdx^{4cv} mice showed a smaller change in activity in anticipation of the start of the dark phase, compared to WT mice. D) Long movement threshold values revealed decreases in threshold for both mdx and mdx^{4cv} mice compared to WTs E) Maximum velocity of long movement segment was decreased in mdx compared to WT mice. F) Long movement arrest threshold was significantly lower in mdx mice compared to WTs. Asterisks indicate * P<0.05, ** P<0.01, *** P<0.001. Cartoons are taken from Loos et al. 2014.*

Movement and arrest segments were identified and duration and distance traveled were determined for each segment. Frequency plots were made for the distance traveled during each movement. On these plots, 2 Gaussian curves were fitted and thresholds were determined by the intersection of the two curves, as described in Loos et al (Loos et al. 2014)(Fig. 5D-F). Both *mdx* and *mdx^{4cv}* mice showed decreased long movement threshold values compared to WT (P<0.001 for both) (Fig 5D). Furthermore, *mdx* mice showed a lower maximum velocity in the long movement segments compared to WTs (P=0.007) (Fig. 5E). For the duration of each arrest, only one Gaussian curve was fitted and the threshold was determined by calculating the 90 percentile of the area under the fitted curve. This threshold, to separate short and long arrest segments, was reduced in *mdx* mice compared to WTs (P=0.021) (Fig 5F). Altogether these changes indicate an altered movement pattern being most prominently in *mdx* mice.

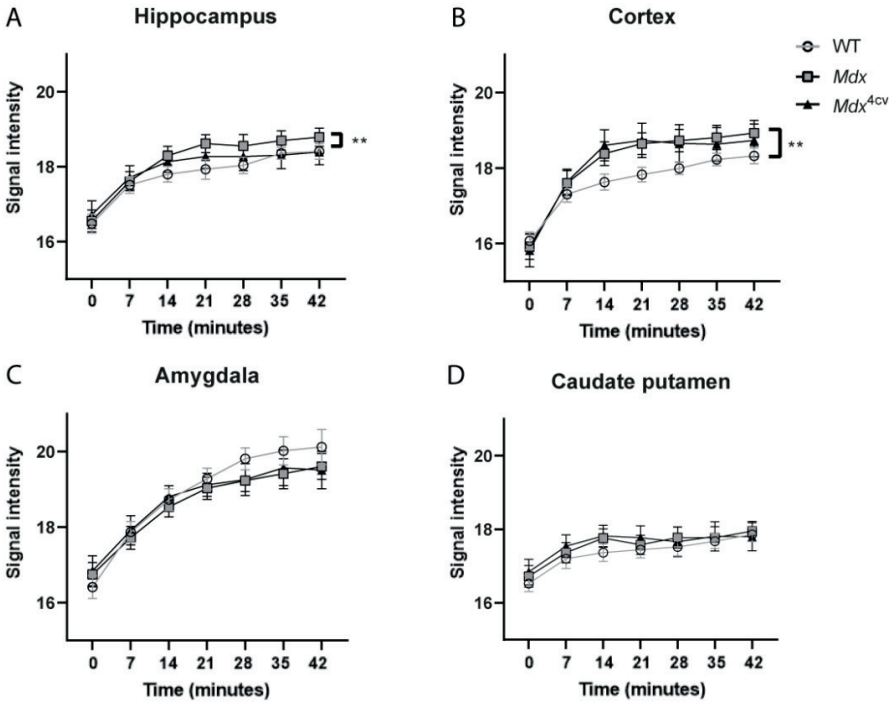

Figure 6: Blood-brain barrier permeability in WT (n=10), mdx (n=9) and mdx^{4cv} (n=10) mice. *A) Signal intensity of the hippocampus. Mdx mice had increased T1 values compared to WTs. B) Signal intensity of the cortex. Mdx^{4cv} mice showed increased T1 values compared to WTs. C) Signal intensity of the amygdala. D) Signal intensity of the caudate putamen. Asterisks indicate ** P<0.01.*

Decreased blood-brain barrier integrity in the hippocampus and cortex in DMD mouse models

The blood-brain barrier (BBB) is an important structure in the brain and its integrity is known to be affected in *mdx* mice (Nico et al. 2003). To determine if BBB alterations are similar between DMD models, BBB permeability was analyzed by *in vivo* MRI. Prior to sacrifice, *in vivo* MRI was used to image brain structure and to assess BBB integrity. Additionally, volumes of the total brain and 23 specific regions were assessed and compared between the strains. No differences in volume were found in any of the brain regions between strains (Table S4).

To determine the BBB integrity, mice were scanned at baseline and at six subsequent one minute intervals after intraperitoneal injection of the contrast solution gadoteridol. One *mdx* mouse was excluded from the analysis due to abnormally

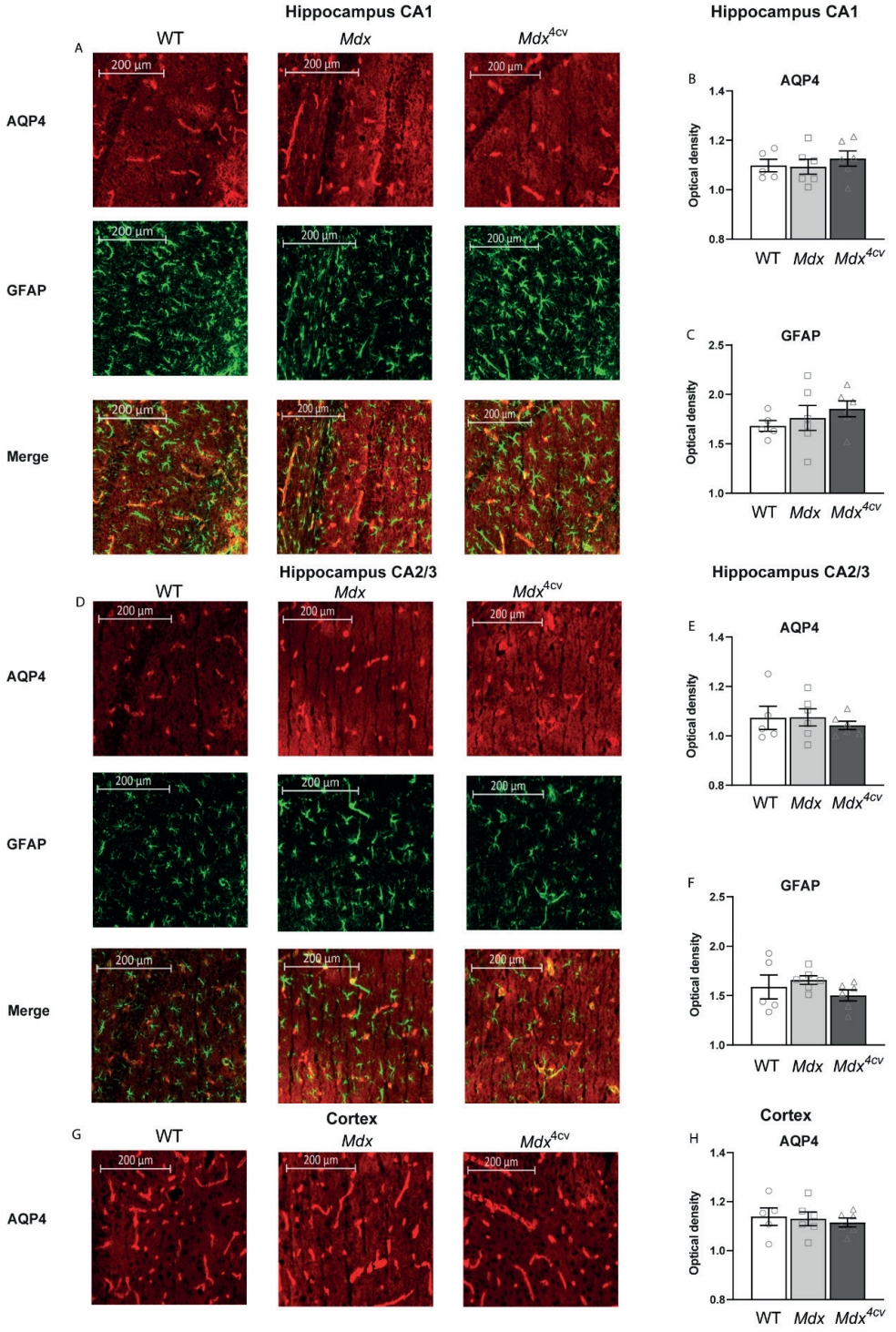
Hippocampus CA1
WT
Mdx
Mdx4cv
A
AQP4
GFAP
Merge
200 µm
Hippocampus CA1
B
AQP4
Optical density
1.4
1.2
1.0
0.8
WT Mdx Mdx4cv
C
GFAP
2.5
2.0
1.5
1.0
Hippocampus CA2/3
D
E
F
Cortex
G
H

Figure 7: immunohistochemical staining quantification of AQP4 and GFAP in WT (n=5), mdx (n=6) and mdx^{4cv} (n=6) mice. *A) Representative images of AQP4 and GFAP expression in the CA1 region of the hippocampus of a WT, mdx and mdx^{4cv} mouse. B) No significant differences in expression levels of AQP4 in the CA1 region of the hippocampus. C) No significant differences in expression levels of GFAP in the CA1 region of the hippocampus. D) Representative images of AQP4 and GFAP expression in the CA2/3 region of the hippocampus of a WT, mdx and mdx^{4cv} mouse. E) No significant differences in expression levels of AQP4 in the CA2/3 region of the hippocampus. F) No significant differences in expression levels of GFAP in the CA2/3 region of the hippocampus. G) Representative images of AQP4 expression in the cortex of a WT, mdx and mdx^{4cv} mouse. H) No significant differences in expression levels of AQP4 in the cortex. I) Representative image of a WT mouse, showing the location of the ROIs drawn for each region.*

high values (> 2 STDs higher than average) in multiple regions. Linear mixed models were used to assess the influence of mouse strains on timelapses for BBB integrity for the hippocampus, cortex, amygdala and caudate putamen, as these areas have high dystrophin expression levels in WT mice (Fig. 6). *Mdx* mice showed increased BBB permeability in the hippocampus (P=0.007) and in the cortex (P=0.058), reaching only significance in the hippocampus (Fig. 6A-B). *Mdx^{4cv}* mice had increased permeability in the cortex compared to WT mice (P=0.007), but not in the hippocampus. Permeability in the amygdala was lower in both DMD strains compared to WT, but this did not reach significance (P = 0.058) (Fig. 6C). No differences were found in permeability in the caudate putamen (Fig. 6D).

To confirm MRI observations, immune-fluorescence stainings for aquaporin 4 (AQP4), a channel that enhances water flux in the brain, and glial fibrillary acidic protein (GFAP), a hippocampal astrocyte marker, were done on cryosections of 6 mice per group. Overall expression intensity was determined in hippocampus CA1 and CA3 regions for both AQP4 and GFAP, and in the cortex for AQP4, however no differences were found in any of the regions (Fig 7). One WT mouse had to be excluded due to freezing damage of the brain slides.

Discussion

The consequences of a lack of full-length dystrophin on the brain in *mdx* mice have been investigated by numerous studies. They provided us with a wide variety of affected cognitive processes, including learning and memory, but research focusing on the consequences of cumulative loss of distinct dystrophin isoforms in the brain is sparse. This study aimed to unravel these consequences on cognition and brain pathology, focusing on spontaneous behavior, different types of learning and mem-

ory, anxiety and blood-brain barrier pathology. Some of the tests conducted are known to show only mild deficits in *mdx* mice, but they were deliberately selected to allow detection of potential additional effects induced by the lack of Dp140. Using behavioral paradigms and brain analyses previously unexplored in mice lacking Dp140, we showed similar behavior and pathology for *mdx* and *mdx*^{4cv} mice, indicating minimal involvement of Dp140 in processes of spontaneous behavior and different aspects of learning and memory.

Both *mdx* and *mdx*^{4cv} showed decreased alternations in the T-maze, which contradicts with the study of Remmelink et al that used a different protocol in which mice were forced forward with a protruding latch (Remmelink et al. 2016). The decrease in alternation in our current study could indicate a partial deficit in working memory, however other factors, such as anxiety, could have influenced the alternation patterns. *Mdx* mice, and mice lacking Dp140 in addition, have increased anxiety (Manning et al. 2014, Remmelink et al. 2016, Vaillend and Chaussenot 2017, Saoudi et al. 2021), which could have led to a preference for the previously explored areas. However, performance was consistent between trials, suggesting minimal involvement of habituation or stress due to repeated exposure. It should be noted that we did not find increased anxiety in our study using the light bulb test in the PhenoTyper cages, however since WT mice drastically minimized their exposure to the stimulus during this test, it was almost impossible to reach even lower levels for the DMD models. Therefore, the lack of difference in anxiety in our study is most likely due to a suboptimal methodology, in which the lux of the lamp was probably too high, and does not directly contradict earlier research on increased anxiety in mice lacking Dp427 and Dp140 (Saoudi et al. 2021).

During the spatial learning phase in the MWM test, *mdx* mice showed a decreased learning curve, indicating a delay, but not a total deficit in spatial learning. They also experienced more difficulty with swimming, as indicated by their decreased velocity, and thus stress which could have affected their learning potential. Previous studies, using a similar protocol, however, failed to show this delay in spatial learning in *mdx* mice even though they did observe lower swimming velocity (Sesay et al. 1996, Vaillend et al. 2004). It remains unclear why the decreased spatial learning was not observed in *mdx*^{4cv} mice. The MWM test is heavily reliant on muscle performance, and even though we tried to compensate for this by excluding parameters related to swim speed, like latency, we cannot rule out that stress or fatigue has influenced the results. Therefore, it would be beneficial to further investigate spatial learning and memory in a less demanding task in terms of motor function.

In contrast to the decreased performance in working and spatial memory, *mdx* and *mdx*^{4cv} mice outperformed WTs in a food rewarded discrimination learning task, which we had not observed in earlier studies (Remmelink et al. 2016, Engelbeen et al. 2021). Increased performance in food motivated tasks has been observed in *mdx*

mice before (Lewon et al. 2017). This likely results from an increased food drive derived from their skeletal muscle hypertrophy induced increased metabolic demand. Interestingly, this did not affect learning capacity during the reversal learning test.

It could be argued that the lack of outperformance of WTs would be counterbalanced by a learning flexibility delay in *mdx* mice. However, lack of evidence on deficits in reversal learning in *mdx* mice in the MWM, makes this hypothesis unlikely. Deficits in fear-learning, which is heavily dependent on the amygdala (Phillips and LeDoux 1992) have been studied before in *mdx* and *mdx52* mice, lacking Dp427 and Dp140 (Saoudi et al. 2021). Spatial learning and spontaneous alterations are less dependent on amygdala involvement, but more on the hippocampus (Douglas and Isaacson 1964, Silvers et al. 2003). This suggests that learning and memory deficits caused by the lack of Dp140 are mostly dependent on the amygdala.

Spontaneous behavior was assessed in the PhenoTyper cages, using 24h automated tracking. All parameters were subtracted from the exact same time windows during the day to minimize influences of circadian rhythm on muscle performance (Gao et al. 2020, Betts et al. 2021). Spontaneous activity of *mdx* and *mdx*^{4cv} mice was mostly altered in terms of movement and arrest patterns and activity, which are heavily influenced by muscle function. Interestingly, this effect seemed more pronounced in *mdx* mice, while literature has shown that the additional lack of Dp140 could further exacerbate motor function (Chesshyre et al. 2022). However, it should be noted that the difference between *mdx* and *mdx*^{4cv} mice was minimal. Since other aspects of spontaneous behavior, like sheltering behavior and habituation, were unaffected, the differences in movement and activity are most likely secondary to muscle fatigue and do not directly point to CNS involvement. However, these results do stress the importance of awareness of muscles involvement in behavioral experiments.

BBB permeability was increased in both *mdx* and *mdx*^{4cv} mice, however not in the same manner. While *mdx* mice showed decreases in BBB integrity in the hippocampus and a trend in the cortex, only the cortex was affected in *mdx*^{4cv} mice. Even though BBB permeability has not been studied before in this manner in *mdx* mice, it is known that the structure and the development of the BBB is affected in these mice and that mice suffer from abnormal cerebral diffusion and perfusion (Goodnough et al. 2014). Literature has shown alterations in expressions of multiple proteins associated with BBB integrity or development, including a reduction of AQP4 and GFAP (Frigeri et al. 2001, Nico et al. 2003, Nicchia et al. 2004, Vajda et al. 2004). Interestingly, we could not detect decreases in AQP4 nor GFAP levels in our study. Confirmation of immunohistochemical results by other types of protein quantifications would be desired, however lack of tissue samples prohibits further investigations. Furthermore, the age of the mice could influence the inconsistencies between our study and literature and deviations in AQP4 or GFAP expression at other time

points cannot be ruled out. It should be noted that Dp71, a shorter dystrophin isoform that is still present in both *mdx* and *mdx*^{4cv} mice is known to interact with AQP4 clustering. While AQP4 does not seem to be the main player in BBB permeability in our study, it could be affected and influencing cognition in DMD models lacking the shorter dystrophin isoforms. Nevertheless, we showed that lack of Dp427 can affect the functioning of the BBB, resulting in increased permeability in multiple regions, while Dp140 does not seem to have an added effect on BBB permeability in our model. While both *mdx* and *mdx*^{4cv} mice lack different dystrophin isoforms, the expression of Dp71 and Dp40 remains unaffected. It is known that DMD patients with mutations affecting these shorter isoforms suffer from more severe behavioral and cognitive deficits (Taylor et al. 2010, Ricotti et al. 2016). It would be of interest to investigate the additional effects of the loss of Dp71 and Dp40 in mice in the future.

Conclusion

Overall we confirmed earlier research in *mdx* mice showing partial deficits in different learning domains and showed that they do not have CNS related deviations in spontaneous behavior. Lack of Dp140 is known to increase anxiety and cause deficits in fear learning. However the additional lack of Dp140 in *mdx*^{4cv} mice did not lead to substantial differences compared to *mdx* mice in any of our tests, indicating a minimal or no role of Dp140 in tasks related to different types of hippocampal dependent memory or spontaneous behavior. Whether Dp140 plays a role in other cognitive processes has yet to be determined.

Ethical statement

The animal study was reviewed and approved by Central Authority for Scientific Procedures on Animals and performed according to Dutch regulation for animal experimentation, and in accordance with EU Directive 2010/63/EU.

Competing interests

None related to this work. For full transparency, AAR discloses being employed by LUMC, which has patents on exon skipping technology, some of which has been licensed to BioMarin and subsequently sublicensed to Sarepta. As co-inventor of some of these patents AAR is entitled to a share of royalties. AAR further discloses being ad hoc consultant for PTC Therapeutics, Sarepta Therapeutics, Regenxbio, Alpha Anomeric, Lilly BioMarin Pharmaceuticals Inc., Eisai, Entrada, Takeda, Splic-

esense, Galapagos, MitoRx and Astra Zeneca. Past ad hoc consulting has occurred for: CRISPR Therapeutics, Summit PLC, Audentes Santhera, Bridge Bio, Global Guidepoint and GLG consultancy, Grunenthal, Wave and BioClinica. AAR also reports having been a member of the Duchenne Network Steering Committee (BioMarin) and being a member of the scientific advisory boards of Eisai, hybridize therapeutics, silence therapeutics, Sarepta therapeutics. Past SAB memberships: ProQR, Philae Pharmaceuticals. Remuneration for these activities is paid to LUMC. LUMC also received speaker honoraria from PTC Therapeutics, Alnylam Netherlands, Pfizer and BioMarin Pharmaceuticals and funding for contract research from Italfarmaco, Sapreme, Eisai, Galapagos, Synnaffix and Alpha Anomeric. Project funding is received from Sarepta Therapeutics and Entrada.

Funding

This project was funded by Duchenne Parent Project-NL and Belgium grant 15.003.

Acknowledgements

We would like to acknowledge Max Gentenaar for his help with the histology and Pietro Spitali for generating a data analysis script.

Author contributions

M. Verhaeg: Investigation, Software, Formal analysis, writing – original draft, writing- review & editing, visualization, K. Adamzek: Methodology, Investigation D. van de Vijver: Investigation K. Putker: Investigation S. Engelbeen: Investigation D. Wijnbergen: Software M. Overzier: Investigation E. Suidgeest: Investigation L. van der Weerd: Supervision, Validation A. Aartsma-Rus: Conceptualization, Validation, Resources, writing- review & editing, supervision, project administration M. van Putten: Conceptualization, Methodology, writing- review & editing, supervision, funding acquisition

Supplementary data

Table S1: Overview statistical tests per parameter. *MWM: Morris water maze, BBB: blood brain barrier, AQP4: aquaporin 4. GFAP: Glial fibrillary acidic protein*

	Parameter	Comparison	Test
T-maze	Alternation	Between groups	Kruskal-Wallis Mann-Whitney repeated tests
		Chance level (0.5)	One-sample Wilcoxon signed-rank test
		Between trials	Linear mixed models
MWM - spatial learning	Distance to platform	Between groups	Linear mixed models (reference: day 1)
	Maximum velocity	Between groups	Tukey HSD
	Relative distance in target quadrant	Chance level (0.25)	One sample t-test
MWM - reversal learning	Distance to platform	Between groups	Linear mixed models (reference: day 1)
	Maximum velocity	Between groups	Tukey HSD
	Relative distance in target quadrant	Chance level (0.25)	One sample t-test
PhenoTyper - Spontaneous behavior	Activity duration - light	Between groups	Kruskal-Wallis
	Mean activity duration - light	Between groups	Kruskal-Wallis Mann-Whitney repeated tests
	Activity duration - dark/light index	Between groups	Kruskal-Wallis
	Activity duration dark	Between groups	Tukey HSD
	Mean activity duration - dark	Between groups	Tukey HSD
	Activity duration - Habituation ratio light	Between groups	Kruskal-Wallis
		Chance level (1)	One-sample Wilcoxon signed-rank test
	Activity duration - Habituation ratio dark	Between groups	Tukey HSD
		Chance level (1)	One sample t-test
	Activity change in anticipation of dark	Between groups	Kruskal-Wallis Mann-Whitney repeated tests
		Chance level (0)	One-sample Wilcoxon signed-rank test
	Activity change in response to dark	Between groups	Kruskal-Wallis
		Chance level (0)	One-sample Wilcoxon signed-rank test
	Activity change in anticipation of light	Between groups	Kruskal-Wallis
		Chance level (0)	One-sample Wilcoxon signed-rank test
	Activity change in response to light	Between groups	Kruskal-Wallis
		Chance level (0)	One-sample Wilcoxon signed-rank test

	Short shelter visit threshold	Between groups	Tukey HSD
	Long shelter visit threshold	Between groups	Tukey HSD
	Long shelter visit fraction of total visits	Between groups	Kruskal-Wallis
	Long shelter visit duration – dark	Between groups	Tukey HSD
	Onshelter zone number – dark	Between groups	Tukey HSD
	Long arrest threshold	Between groups	Kruskal-Wallis Mann-Whitney repeated tests
	Mean long arrest duration – light	Between groups	Kruskal-Wallis Mann-Whitney repeated tests
	Long movement threshold	Between groups	Turkey HSD
	Long movement max velocity	Between groups	Turkey HSD (log transform)
	velocity dark 2	Between groups	Tukey HSD
	velocity light 2	Between groups	Tukey HSD
PhenoTyper - Anxiety	Proportion of time outside shelter	Between groups and conditions	Linear mixed models
PhenoTyper - Discrimination learning	Entries till 80% succes rate	Between groups	Martel-cox test of survival curves
PhenoTyper - Reversal learning	Entries till 80% succes rate	Between groups	Martel-cox test of survival curves
MRI - BBB integrity	Hippocampus	Between groups and time	Linear mixed models
	Cortex	Between groups and time	Linear mixed models
	Amygdala	Between groups and time	Linear mixed models
	Caudate putamen	Between groups and time	Linear mixed models
AQP4 and GFAP staining	Mean grey area values	Between groups	Turkey HSD

Table S2: Overview of statistical parameters. *Additional statistical parameters reported in case of significant differences (P < 0.05).*

	Parameter	Comparison	*P*-value	Additional statistical values
T-maze	Alternation – chance level	*Mdx*	*P* = 0.017	Z = 2.939
		Mdx^{4cv}	*P* < 0.001	Z= 3.568
	Alternations – between groups	*Mdx* vs WT	*P* < 0.001	Z = -3.483
		Mdx^{4cv} vs WT	*P* = 0.007	Z = -2.701
MWM – Spatial learning	Distance to platform	Trial effect	*P* < 0.001	F(1,275) = 253.4
		Mdx vs WT	*P* = 0.002	F(1,273) = 9.38
		Mdx vs *Mdx*^{4cv}	*P* = 0.003	F(1,273) = 9.08
	Maximum velocity	*Mdx* vs WT	*P* < 0.001	F(1,66) = 49.9
		Mdx vs *Mdx*^{4cv}	*P* < 0.001	F(1,66) = 22.24
MWM – Reversal learning	Maximum velocity	*Mdx* vs WT	*P* < 0.001	F(1,66) = 45.0
		Mdx vs *Mdx*^{4cv}	*P* < 0.001	F(1,66) = 46.3
PhenoTyper - Discrimination learning	Entries till 80% succes rate	*Mdx* vs WT	*P* = 0.032	Hazard ratio = 1.784
		Mdx^{4cv} vs WT	*P* = 0.006	Hazard ratio = 2.070
PhenoTyper - Anxiety	Time outside shelter – anxiety response vs baseline	*Mdx*	*P* < 0.001	F(1,263) = 15.3
		Mdx^{4cv}	*P* = 0.002	F(1,305) = 9.4
		WT	*P* < 0.001	F(1,277) = 37.3
PhenoTyper - Spontaneous behavior	Velocity dark	Strain comparison (one-way ANOVA)	*P* = 0.017	F(2,63) = 2.361
	Activity duration dark	Strain comparison (one-way ANOVA)	*P* = 0.004	F(2,63) = 5.923
	Activity change - Anticipation to dark	*Mdx* vs WT	*P = 0.001*	Z = -3.207
		Mdx^{4cv} vs WT	*P* = 0.041	Z = -2.042
	Long movement threshold	Strain comparison (one-way ANOVA)	*P* < 0.001	F(2,63) = 20.10
	Long movement – maximum velocity	Strain comparison (one-way ANOVA)	*P* = 0.011	F(2,63) = 4.901
	Long arrest threshold	*Mdx* vs WT	*P* = 0.021	Z = -2.284
MRI – BBB integrity	Hippocampus	*Mdx* vs WT	*P* = 0.007	F(1,171) = 6.9
		Mdx^{4cv} vs WT	*P* = 0.007	F(1,171) = 6.7
	Cortex	*Mdx* vs WT	*P* = 0.058	F(1,171) = 3.5
	Amygdala	Strain effect	*P* = 0.058	F(2,177) = 2.88

Table S3: Overview of behavioral parameters and P-values of spontaneous behavior in PhenoTyper cages. *Parameters for mean activity duration were not taken along due to irregularities in calculations caused by flickering of the camera. P-values were adjusted with false discovery rate. If P < 0.05, Additional statistical values are given*

Parameter	Statistical test	*P*-value ANOVA	*Mdx* vs wt	*Mdx*^{4cv} vs wt	*Mdx* vs *mdx*^{4cv}
Activity duration - light	Kruskal-Wallis	*P* = 0.178			
Activity duration – dark/light index	Kruskal-Wallis	*P* = 0.665			
Activity duration - dark	Tukey HSD	*P* = 0.004	*P* = 0.008	*P* = 0.015	*P* = 0.974
Activity duration - habituation ratio light	Kruskal-Wallis	*P* = 0.795			
Activity duration - habituation ratio dark	Tukey HSD	*P* = 0.060			
Activity change in anticipation of dark	Kruskal-Wallis and Mann-Whitney repeated tests	*P* = 0.036	*P* = 0.001	*P* = 0.041	*P* = 0.650
Activity change in response to dark	Kruskal-Wallis	*P* = 0.474			
Activity change in anticipation of light	Kruskal-Wallis	*P* = 0.650			
Activity change in response to light	Kruskal-Wallis	*P* = 0.372			
Short shelter visit threshold	Tukey HSD	*P* = 0.058			
Long shelter visit threshold	Tukey HSD	*P* = 0.107			
Long shelter visit fraction of total visits	Kruskal-Wallis	*P* = 0.795			
Long shelter visit duration – dark	Tukey HSD	*P* = 0.966			
Onshelter zone number – dark	Tukey HSD	*P* = 0.861			
Long arrest threshold	Kruskal-Wallis and Mann-Whitney repeated tests	*P* = 0.036	*P* = 0.021	*P* = 0.123	*P* = 0.482
Mean long arrest duration – light	Kruskal-Wallis and Mann-Whitney repeated tests	*P* = 0.676			
Long movement threshold	Turkey HSD	*P* = 0.001	*P* = 0.001	*P* = 0.001	*P* = 0.146
Long movement max velocity	Turkey HSD (log transform)	*P* = 0.011	*P* = 0.007	*P* = 0.281	*P* = 0.255
Velocity dark	Tukey HSD	*P* = 0.017	*P* = 0.012	*P* = 0.254	*P* = 0.459
Velocity light	Tukey HSD	*P* = 0.676			

Table S4: Volumetric analysis in WT (n=10), mdx (n=9) and mdx^{4cv} (n=10) mice. *No significant differences were found between groups in any of the brain areas. P-values are adjusted for multiple comparison using false discovery rate. Std: Standard deviation*

Area	WT		*Mdx*		*Mdx^{4cv}*		*P*-value
	Average	STD	Average	STD	Average	STD	
Total brain volume	452.31	14.28	452.99	16.93	444.03	15.28	0.636
Hippocampus	29.12	1.44	29.51	2.29	28.76	1.25	0.744
Corpus callosum	16.07	0.59	16.21	1.04	16.08	0.68	0.940
Caudate putamen	25.03	1.32	25.60	0.92	24.91	1.01	0.636
Anterior commisure	1.35	0.17	1.19	0.14	1.30	0.17	0.441
Globus pallidus	2.35	0.21	2.39	0.10	2.33	0.13	0.744
Internal capsule	4.16	0.29	4.19	0.32	4.31	0.29	0.697
Thalamus	25.50	1.11	25.57	1.15	24.88	0.85	0.636
Cerebellum	51.51	1.38	53.97	3.92	52.79	3.02	0.636
Superior colliculus	8.05	0.42	8.03	0.78	7.68	0.46	0.636
Ventricles	7.15	0.80	7.30	1.02	6.77	0.86	0.636
Hypothalamus	12.89	0.71	13.35	0.49	12.44	0.66	0.264
Inferior colliculus	4.63	0.13	4.66	0.33	4.55	0.30	0.744
Periaqueductal gray	3.29	0.17	3.37	0.47	3.28	0.24	0.872
Cortex	87.05	2.61	85.98	4.45	84.98	2.07	0.636
Amygdala	11.43	0.32	10.97	0.40	11.18	0.36	0.312
Olfactory bulb	25.71	1.40	23.40	2.04	23.63	2.81	0.368
Hind brain	49.39	2.98	49.47	2.89	48.96	4.36	0.940
Reticular nucleus	12.64	0.67	13.06	0.77	12.27	0.77	0.425
Nucleus accumbens	16.79	0.91	17.14	0.86	16.29	0.87	0.464
Fimbria	1.41	0.08	1.50	0.20	1.43	0.14	0.636
Cingulate	3.76	0.26	3.82	0.38	3.59	0.35	0.636
Motor cortex	17.08	1.09	16.79	1.12	16.46	1.27	0.697
Sensory motor cortex	30.86	1.28	30.50	1.46	30.18	0.32	0.636

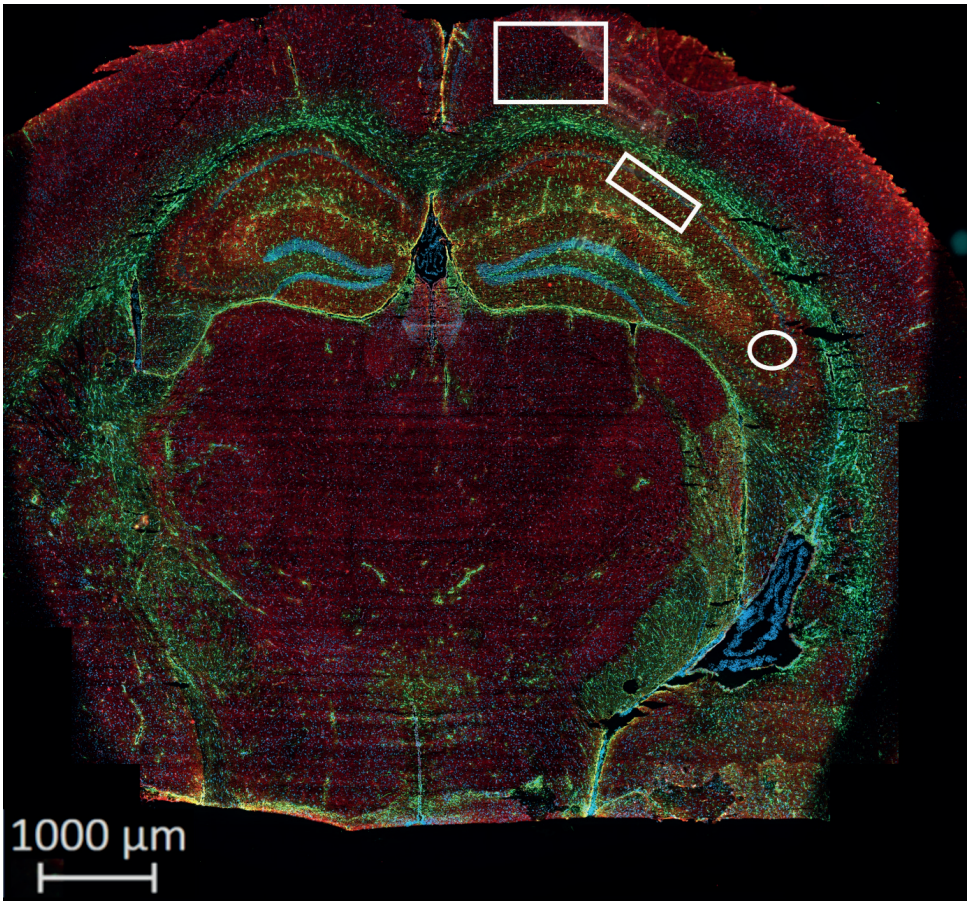

Figure S1: Overview of ROI regions of AQP4 and GFAP staining. *ROI regions of the cortex (1), hippocampus CA1 (2) and CA2/3 (3) region)*